

# Ultrahigh-resolution pyroelectric thermal-wave technique for the measurement of thermal diffusivity of low-concentration water-alcohol mixtures

Anna Matvienko and Andreas Mandelis<sup>a)</sup>

*Center for Advanced Diffusion-Wave Technologies, Department of Mechanical and Industrial Engineering, University of Toronto, Toronto M5S 3G8, Canada*

(Received 13 July 2005; accepted 25 August 2005; published online 5 October 2005)

Thermal diffusivities of water-methanol and water-ethanol mixtures were measured using a thermal-wave cavity with two techniques: conventional single-pulse photopyroelectric frequency scans and the common-mode-rejection demodulation dual-pulse scheme. The frequency-scan measurements showed maximum resolution of the photothermal signal in water at the level of 0.5% by volume in mixtures of methanol and ethanol. The common-mode-rejection demodulation method improved the resolution up to the level of 0.2% by volume, which is the highest thermophysical resolution of water-methanol and water-ethanol mixtures reported to date, to our best knowledge. The ultrahigh sensitivity of the method can be especially useful in environmental applications, specifically in real-time water pollution monitoring. © 2005 American Institute of Physics.  
[DOI: 10.1063/1.2074627]

## I. INTRODUCTION

In a variety of industrial processes, it is essential to have reliable thermal-diffusivity data of liquids and liquid mixtures in order to design and improve heat and mass transfer instrumentation. Moreover, when dealing with low-concentration mixtures, the high-resolution measurements of thermal properties become very relevant as a tool for pollution detection. In recent years, numerous optical and photothermal methodologies have been successfully employed for the measurement of the thermal diffusivity of aqueous solutions.<sup>1-7</sup> However, to date there has been no thermophysical method accurate enough to study the thermal transport property (i.e., thermal diffusivity) of liquid mixtures at the very low end of concentrations. The lowest concentration reported using thermal lens spectroscopy is 28% w/w for water-methanol mixtures.<sup>1</sup> The thermal-wave interferometric technique is limited to 24.5% w/w resolution for water-glycerin mixtures.<sup>2</sup> The thermal diffusivity of water-methanol and water-ethanol mixtures was obtained using a thermal grating technique with 20% w/w minimal concentration resolution.<sup>3</sup> The same technique allowed measurements of water-calcium chloride and water-magnesium chloride mixtures with a resolution of 5% w/w.<sup>4,5</sup> Recent applications of the thermal-wave cavity technique in the cavity length scan mode to the water-methanol system dramatically improved the accuracy of thermal-diffusivity measurements up to 0.44% w/w concentration of methanol in water and 0.35% w/w of sodium chloride in water.<sup>6</sup> In this case, however, the measurements for the series of mixtures were limited by irreproducibility due to the moving (mechanical) parts of the sensor. In our previous study,<sup>7</sup> we introduced a new design of

the measurement cell with fixed dimensions operating in a frequency-scan mode that allowed measurements of a series of water mixtures. Nevertheless, the highest possible resolution remained unchanged at the level of 0.44% w/w (0.5% v/v) concentration of methanol in water.

The main goal of the present study is to develop a sensitive ultrahigh-resolution thermal-wave cavity technique for thermal-diffusivity measurements of a series of water-alcohol mixtures at the very low end of concentrations with the application of a common-mode-rejection demodulation scheme. The classic thermal-wave cavity method<sup>8</sup> is very simple and inexpensive but limited in sensitivity due to the dynamic range and noise floor of conventional lock-in amplifier demodulation systems. Recent applications of the common-mode-rejection demodulation scheme to the measurements of thermal diffusivity of liquids<sup>9</sup> using the thermal-wave cavity show a substantial improvement in the dynamic range of the instrumental detection. The common-mode-rejection demodulation technique<sup>10,11</sup> involves the launching of two pulses over one modulation period. In this case, the lock-in amplifier output basically represents the difference between the response waves produced by each of the two pulses. This differential technique overcomes the limitations of conventional single square-wave modulation through its ability to suppress background lock-in amplifier signal base lines. Thus, the common-mode-rejection demodulation can considerably increase the overall measurement resolution and detect relatively small signal variations induced by minute differences in the thermal properties of a sample by use of the full dynamic range of the lock-in amplifier which becomes possible through the suppression of the instrumental base line.

In terms of future applications, the proposed system can eventually be implemented into a self-contained *in situ* liquid pollution/contamination monitor.

<sup>a)</sup> Author to whom correspondence should be addressed; electronic mail: mandelis@mie.utoronto.ca

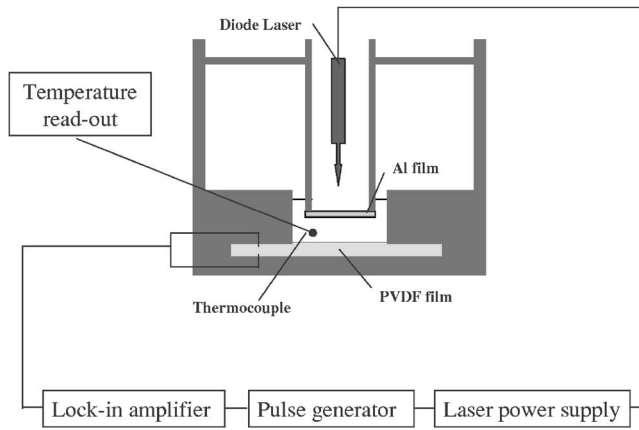


FIG. 1. Experimental setup.

## II. EXPERIMENTAL SETUP

The experimental setup was designed for the measurements of thermal diffusivity of liquid samples (Fig. 1). The setup consisted of a measurement cell, a diode laser ( $\lambda = 809.6$  nm), a laser controller (Coherent, Model 6060), a digital pulse generator (Stanford Research Systems DG535), and a lock-in amplifier (Stanford Research Systems SR830). The intensity of the laser light was modulated using a pulse generator connected to the internal oscillator of the lock-in amplifier. The laser beam was incident on a 100- $\mu\text{m}$ -thick aluminum film, which converted optical waves to thermal waves propagating through the liquid sample. A pyroelectric film [Measurement Specialties, Inc., 52- $\mu\text{m}$ -thick Ni-Al polyvinylidene fluoride (PVDF) film] detected the temperature oscillations in transmission mode and produced an output signal measured by the lock-in amplifier.

The setup was also equipped with a thermocouple, which measured the temperature of the sample during the experiments. The design involved fixed dimensions of the cavity length at a fixed modulation frequency and scanned the common-mode-rejection demodulation wave form pulse for obtaining reproducible measurements with various types of liquid solutions. Data acquisition and device control were automated using the MATLAB software. In this manner, data could be obtained and processed in real time.

It is important to choose the optimal value of the cavity length for mixture measurements: the shorter the cavity length, the better the output signal. At the same time, it is necessary to provide enough intracavity space in order to remove and renew the liquid sample from the cavity, as well as to position a thermocouple to measure the dc temperature of the sample. The main requirement for experiments with a series of water mixtures is that the cavity geometry will not change so that the instrumental transfer function may remain the same during the entire set of measurements. The measurement cell should be constructed with appropriate dimensions commensurate with the thermal diffusion length in the fluid at the chosen frequency, also to allow for changing sample without moving the cavity walls. In this work, we used cavity length  $L=0.5$  mm for the water mixture measurements.

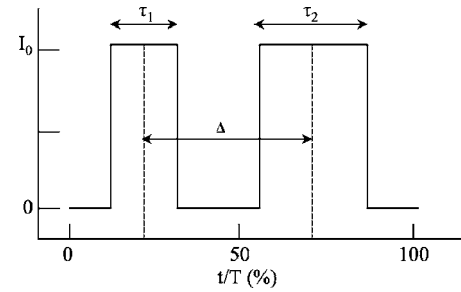


FIG. 2. The two-pulse configuration of the common-mode-rejection demodulation scheme.

## III. THEORETICAL BACKGROUND

The two-pulse configuration of the common-mode-rejection demodulation scheme is shown in Fig. 2. The optical excitation wave form consists of a bimodal pulse applied to the thermal-wave cavity. In the figure, time is expressed as a percentage of the full repetition period  $T$ , while  $\tau_1$  and  $\tau_2$  are the corresponding square pulse widths, and  $\Delta$  is the center-to-center time delay. The methodology consists of launching two pulses of different fixed widths  $\tau_1$  and  $\tau_2$ , separated by center-to-center time delay  $\Delta$  in one modulation period, and monitoring the output signal as a function of the time delay  $\Delta$ .

It has been shown<sup>10</sup> that the real (in phase) and imaginary (quadrature) parts of the demodulated lock-in output  $Y(\omega, \Delta)$  of the experimental system with a bimodal periodic pulse excitation are given by

$$\begin{aligned} \text{Re}[Y(\omega, \Delta)] = & -\frac{2I_0}{\pi} \left\{ \cos\left(\frac{\pi\Delta}{T}\right) \left[ \sin\left(\frac{\pi\tau_1}{T}\right) \right. \right. \\ & \left. \left. + \sin\left(\frac{\pi\tau_2}{T}\right) \right] \text{Re}[V(\omega)] + \sin\left(\frac{\pi\Delta}{T}\right) \right. \\ & \left. \times \left[ \sin\left(\frac{\pi\tau_1}{T}\right) - \sin\left(\frac{\pi\tau_2}{T}\right) \right] \text{Im}[V(\omega)] \right\}, \end{aligned} \quad (1a)$$

$$\begin{aligned} \text{Im}[Y(\omega, \Delta)] = & +\frac{2I_0}{\pi} \left\{ \sin\left(\frac{\pi\Delta}{T}\right) \left[ \sin\left(\frac{\pi\tau_1}{T}\right) \right. \right. \\ & \left. \left. - \sin\left(\frac{\pi\tau_2}{T}\right) \right] \text{Re}[V(\omega)] - \cos\left(\frac{\pi\Delta}{T}\right) \right. \\ & \left. \times \left[ \sin\left(\frac{\pi\tau_1}{T}\right) + \sin\left(\frac{\pi\tau_2}{T}\right) \right] \text{Im}[V(\omega)] \right\}, \end{aligned} \quad (1b)$$

where  $\omega$  is the common-mode-rejection demodulation wave form repetition angular frequency and  $V(\omega)$  is the corresponding signal response of the experimental system to a single pulse at the same frequency. It is possible to balance the two terms in the in-phase and quadrature components for the appropriate values of  $\Delta$  so as to obtain zero magnitude for either one of them. Change in thermal properties of the sample shifts the output zero to a new position along the  $\Delta$  axis. The high sensitivity of the common-mode-rejection demodulation makes it possible to distinguish between two liq-

uids with very similar thermal diffusivity by monitoring the pulse separation  $\Delta$  at which the signal takes on the zero value. The common-mode-rejection demodulation theory permits the direct calculation of thermal-diffusivity coefficients using the obtained  $\Delta$  data for the given parameters  $T$

$=2\pi/\omega$ ,  $\tau_1$ , and  $\tau_2$ . The in-phase or quadrature signal [Eqs. (1)] equals to 0 in this case. The response of the experimental system to a single-pulse excitation  $V(\omega)$  can be calculated according to the thermal-wave cavity conduction-radiation theory:<sup>7</sup>

$$V(\omega) = \frac{S(\omega) \frac{2I_0}{k_w \sigma_w \sigma_p} (1 - e^{-L_p \sigma_p}) (Y_{tp} + X_{tp} e^{-L_p \sigma_p}) \left[ (1 - e^{-2L_w \sigma_w}) \frac{H_e}{k_p \sigma_p} + 2b_{wp} e^{-L_w \sigma_w} \right]}{(1 - e^{-2L_s \sigma_s}) \left[ \frac{H}{k_w \sigma_w} [(1 - e^{-2L_w \sigma_w}) Q_{tp} + (1 + e^{-2L_w \sigma_w}) b_{wp} P_{tp}] - \frac{2H_e}{k_w \sigma_w} e^{-2L_w \sigma_w} P_{tp} \right] + b_{wp} P_{tp} Q_{sw} + Q_{tp} P_{sw}}, \quad (2a)$$

$$\begin{aligned} \sigma_j &= (1 + i) \sqrt{\omega/2\alpha_j}, & X_{ij} &= (1 - b_{ij}) + (1 + b_{ij}) e^{-2L_i \sigma_i}, \\ b_{ij} &= \frac{k_i \sigma_i}{k_j \sigma_j}, & Y_{ij} &= (1 + b_{ij}) + (1 - b_{ij}) e^{-2L_i \sigma_i}, \\ H &= 4\sigma_{SB} \varepsilon_w T_{wdc}^3 T_{wac}, & P_{ij} &= (Y_{ij} + X_{ij} e^{-2L_j \sigma_j}), \\ H_e &= 4\sigma_{SB} \varepsilon_w T_{wdc}^3 \exp(-\Delta\beta L_w), & Q_{ij} &= (Y_{ij} - X_{ij} e^{-2L_j \sigma_j}), \\ \Delta\beta &= \beta_0 - \beta. \end{aligned} \quad (2b)$$

Here subscripts  $s$ ,  $w$ ,  $p$ , and  $t$  stand for aluminum film, liquid sample, pyroelectric film, and aluminum substrate, correspondingly;  $\beta_0$  is the infrared-absorption coefficient of pure water. For the frequency-scan experiments, the instrumental factor  $S(\omega)$  can be experimentally normalized out by taking the ratio of the cavity signal to the photopyroelectric signal produced by direct laser light incident on the pyroelectric sensor. The analytical expression for the voltage in this case can be derived immediately by putting  $L_w=0$ ,  $L_s=0$ ,  $H=0$ , and  $H_e=0$  in Eq. (2a). For the common-mode-rejection demodulation scans, the fitting of the pure water curve with known thermal-diffusivity value gives the real and imaginary parts of the unknown instrumental factor  $S(\omega)$ . The thermal diffusivity of the liquid mixture can then be easily obtained from Eqs. (1) or (2a) using the experimental data on the pulse separation  $\Delta$  at which the common-mode-rejection demodulation in-phase or quadrature takes on the zero value.

#### IV. THERMAL-WAVE CAVITY CHARACTERIZATION AND FREQUENCY-SCAN APPROACH

The first set of experiments consisted of conventional frequency scans for water-ethanol mixtures in the entire concentration range of 0%–100%. The length of the cavity and the unknown thermal properties of the materials used in the cavity construction were determined by fitting a frequency-scan measurement with intracavity air to the thermal-wave cavity conduction-radiation theory,<sup>7</sup> since the thermal-diffusivity coefficient of air is well known.<sup>12</sup> The fitted parameters were further used as known values in the determination of thermal diffusivities of liquid samples.

Frequency-scan experiments with water mixture samples were then performed. We found that the accuracy of the mea-

surements was considerably affected by a number of factors such as the flatness of the aluminum film, the purity of the water samples, the thermal properties of the materials used for setup construction, surrounding vibrations, and especially the fluctuations of ambient temperature. To ensure adequate temperature control, the setup was equipped with a thermocouple with a 0.1 °C resolution, which monitored the mean dc temperature of the sample during the measurements. Furthermore, the integrity of the pyroelectric sensor had to be monitored constantly. The contact of the sensor with water leads to the oxidation of its upper metal layer, which reduces the lifetime of the film and affects the signal substantially.

The main issue in the experiments with low concentration mixtures is the measurement reproducibility. Figures 3(a) and 3(b) depict the results of frequency scans for water-ethanol mixtures of several concentrations (v/v %). Two consecutive measurements of the same concentration (fluid was removed and refilled each time) were performed for every mixture to show the reproducibility and ensure that the difference between the curves of the same concentration does not exceed the difference due to concentration change, especially for the low-concentration region. Results for the concentration range of 0%–1% v/v are presented in Figs. 3(c) and 3(d). In these figures, only the part of the curves in the frequency range of 2.25–2.28 Hz is shown to enhance resolution. The figures show excellent reproducibility and the resolution as low as 0.5% v/v concentration of ethanol in water [Figs. 3(c) and 3(d)]. Our attempt to measure 0.2% concentration mixture did not give sufficient resolution. One can only see minor difference between amplitude curves for 0% and 0.2% concentration [Fig. 3(c)]. Furthermore, the phase curves for 0% and 0.2% concentration are coincident, as shown in Fig. 3(d). Thus, the highest possible resolution of the frequency-scan method is 0.5% v/v of ethanol in water, which agrees with the resolution of frequency scans of water-methanol mixtures determined previously.<sup>7</sup>

Thermal diffusivities of water-ethanol mixtures were obtained by fitting the analytical model [Eq. (2a)] to the frequency-scan data. The thermal parameters used in the fitting are listed in Table I. The obtained diffusivity values versus the concentration of mixtures at temperature  $T=23$  °C are presented in Fig. 4. Another important issue in

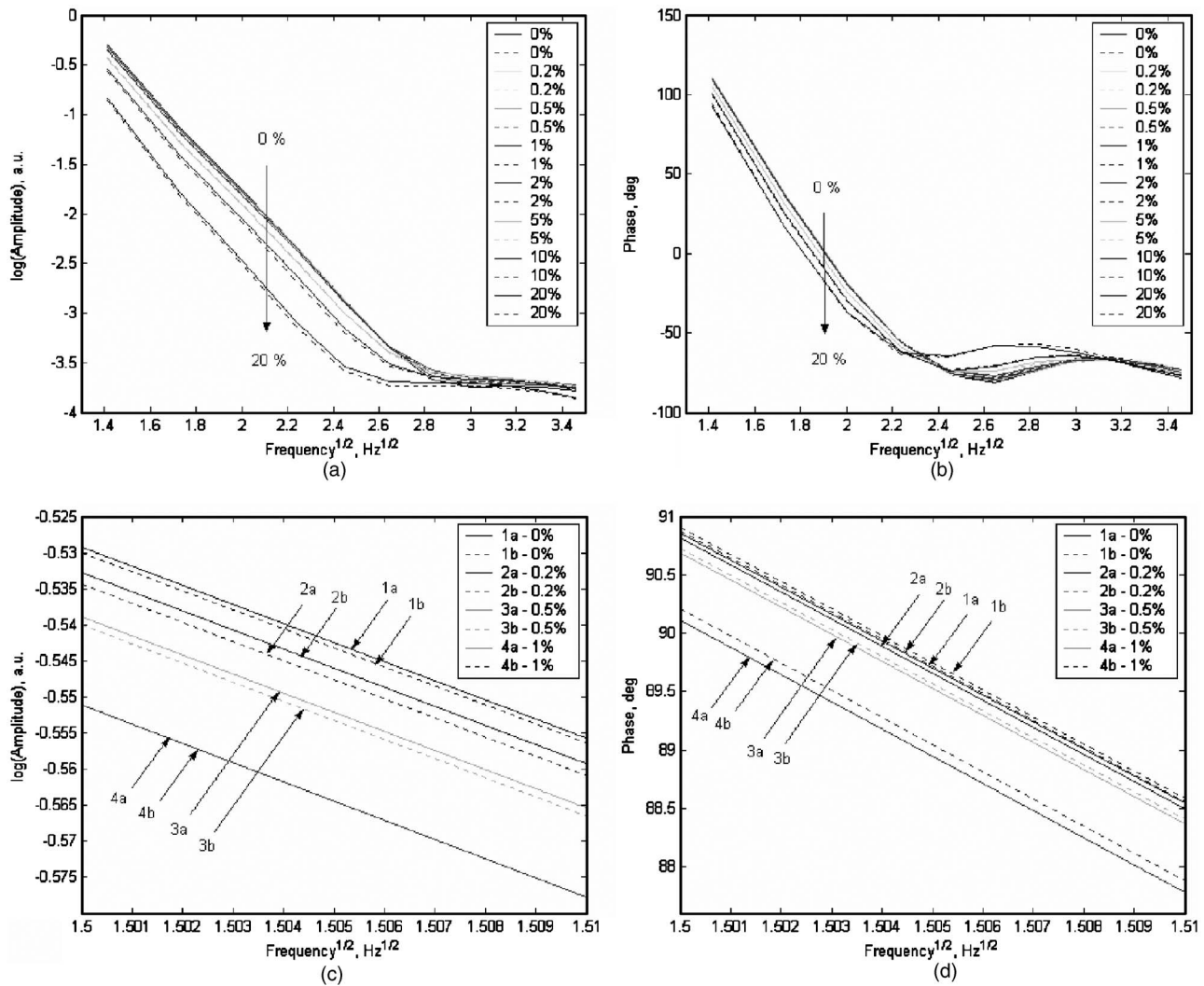


FIG. 3. Frequency-scan amplitudes [(a), (c)] and phases [(b), (d)] for water-ethanol mixtures of different concentrations. Curves [(c), (d)] represent the low-concentration measurements.

the investigation of thermal properties of mixtures is the theoretical description of thermal-diffusivity profiles versus concentration. Figure 4 presents a comparison of the thermal-diffusivity profile measured in this study to the empirical model<sup>7</sup> based on the Jordan correlation<sup>13</sup> for thermal conductivity:

$$\alpha = \frac{k_1^{\nu_1} k_2^{\nu_2} \{\exp[\gamma(k_1 - 3k_2)]\}^{\nu_1 \nu_2}}{\nu_1(k_1/\alpha_1) + \nu_2(k_2/\alpha_2)}, \quad (3)$$

where subscripts (1) and (2) stand for water and ethanol, respectively;  $\gamma$  is an empirical constant;  $\nu_{1,2}$ ,  $\alpha_{1,2}$ , and  $k_{1,2}$  are the volume fractions, thermal diffusivities, and thermal

conductivities of the pure mixture components, respectively; and  $k_1 > k_2$ .

The correlation [Eq. (3)] gives a very good approximation for our data, as seen in Fig. 4. Here, the thermal parameters of water  $\alpha_1 = 1.44 \times 10^{-7} \text{ m}^2 \text{ s}^{-1}$ ,  $k_1 = 0.604 \text{ W m}^{-1} \text{ K}^{-1}$ , and the thermal parameters of ethanol  $\alpha_2 = 0.785 \times 10^{-7} \text{ m}^2 \text{ s}^{-1}$ ,  $k_2 = 0.165 \text{ W m}^{-1} \text{ K}^{-1}$ . The empirical constant  $\gamma$  was the only adjustable parameter and found to be  $-3.08 \text{ m K W}^{-1}$  from the best fit to Eq. (3).

The theoretical model of Eq. (2a) allows the fitting of the infrared emissivity of the mixture as well.<sup>7</sup> However, in the low-frequency range used in these measurements the conduction mechanism substantially prevails over radiation, so that the effects of emissivity on the signal were ignored.

## V. COMMON-MODE-REJECTION DEMODULATION SCHEME

Experiments using the common-mode-rejection demodulation scheme were performed with our liquid samples. The experimental common-mode-rejection demodulation procedure involves the scanning of the lock-in in-phase and

TABLE I. Fitted thermal properties of thermal-wave cavity materials.

	$\alpha$ ( $\text{m}^2 \text{ s}^{-1}$ )	$k$ ( $\text{W m}^{-1} \text{ K}^{-1}$ )
Aluminum film	$8.7 \times 10^{-5}$	28
Pyroelectric film	$7.6 \times 10^{-8}$	0.19
Aluminum substrate	$8.4 \times 10^{-5}$	104

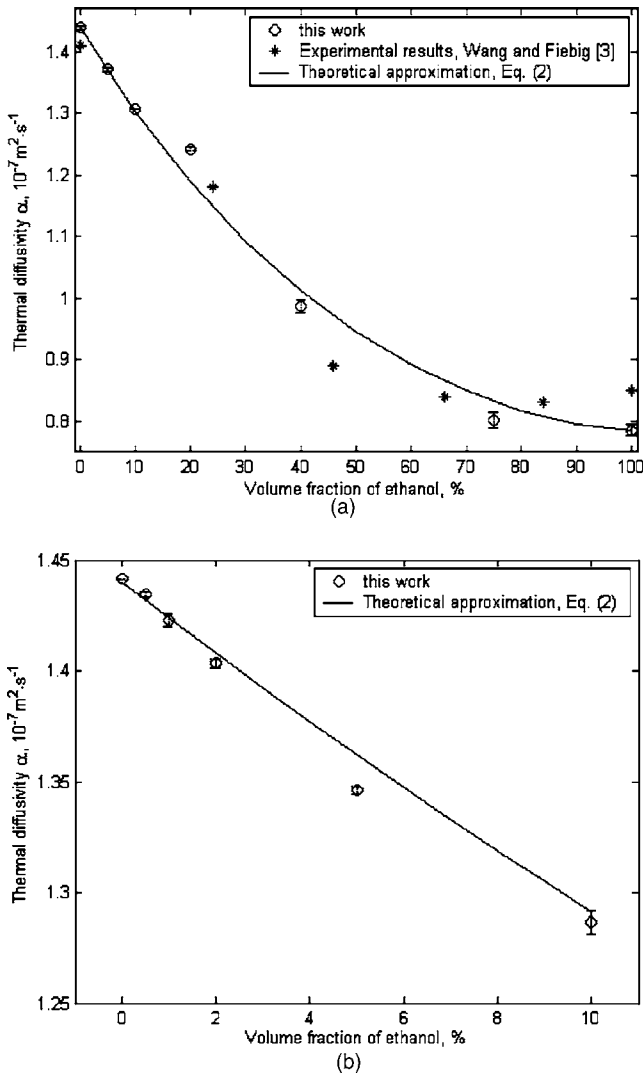


FIG. 4. (a) Thermal diffusivity vs concentration of ethanol in water. (b) Low-concentration measurements. The lines correspond to the best fits to the modified Jordan correlation (Ref. 7). Thermal parameters of the thermal-wave cavity materials are listed in Table I.

quadrature outputs for a given modulation frequency  $f$  as functions of the pulse separation  $\Delta$ . To obtain the best resolution between similar samples, it is necessary that the curve crossing the zero line have the steepest angle. There are several factors that influence the slope of the crossing curve: cavity length, modulation frequency, and thermal properties of the sample. An example of common-mode-rejection demodulation scanning in pure water for various cavity lengths is shown in Fig. 5. One can see that the shorter the cavity length, the higher the amplitude of the output signal, and thus the steeper the angle at the crossing point of the zero line.

The figure also shows the high reproducibility of the measurements. At every cavity length, the measurements were performed twice. Again, the fluid was removed and refilled. The curves at the same cavity length coincide, unlike the case of frequency scans of the same liquids. Therefore, the influence of the sample replacement procedure on the reproducibility of the measurements was found to be negli-

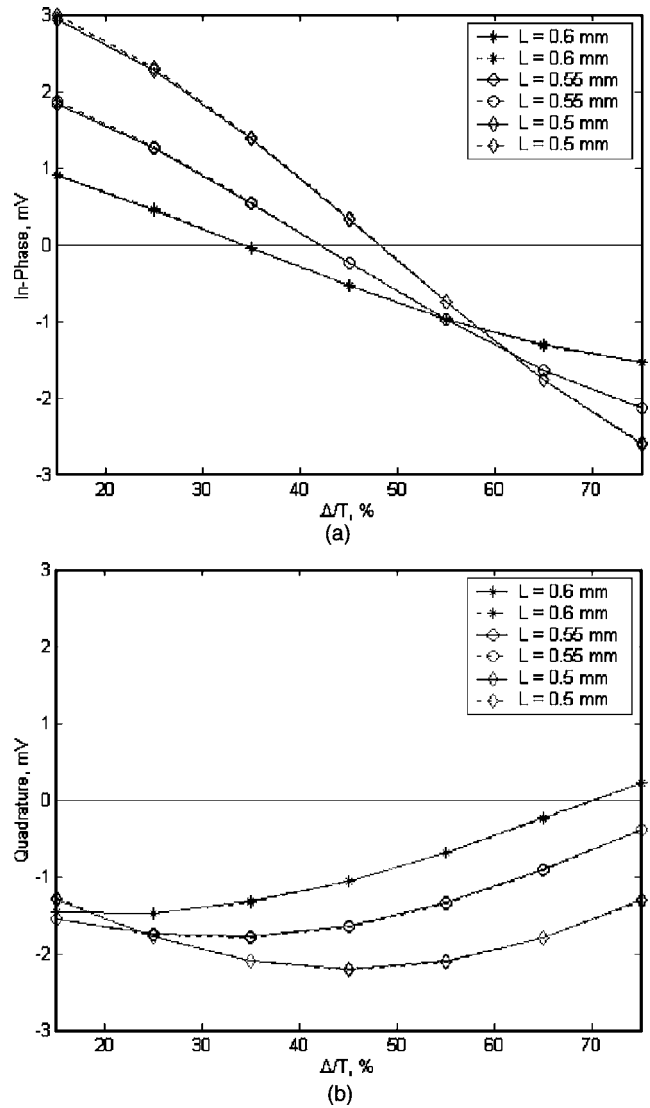


FIG. 5. (a) In-phase and (b) quadrature components of the common-mode-rejection demodulation signal in water for various cavity lengths; modulation frequency  $f = 5 \text{ Hz}$ .

gible. This is the result of using fixed frequency, instead of scanning frequencies, thus avoiding possible instrumental drift.

The signal measured for various modulation frequencies at a fixed cavity length is shown in Fig. 6. An increase in frequency decreases the thermal diffusion length, which leads to decreases in signal strength and crossing angle of the in-phase component.

According to our experiments, the best experimental configuration for a steep crossing angle is a smaller cavity length with a lower frequency. However, at low frequencies the signal becomes very large and temperature stabilization is not attainable within reasonable time. For example, even after 15 consecutive experiments (about 2 h of scanning) with pure water at 3 Hz, the signal for consecutive runs still shifted due to the increased dc temperature of the system. These shifts can be reduced by an optimal choice of the modulation frequency.

To determine an optimally low-drift modulation frequency for applying the common-mode rejection-

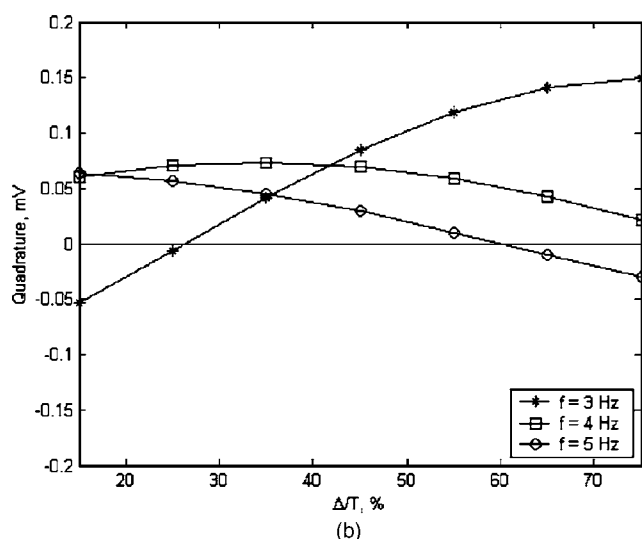
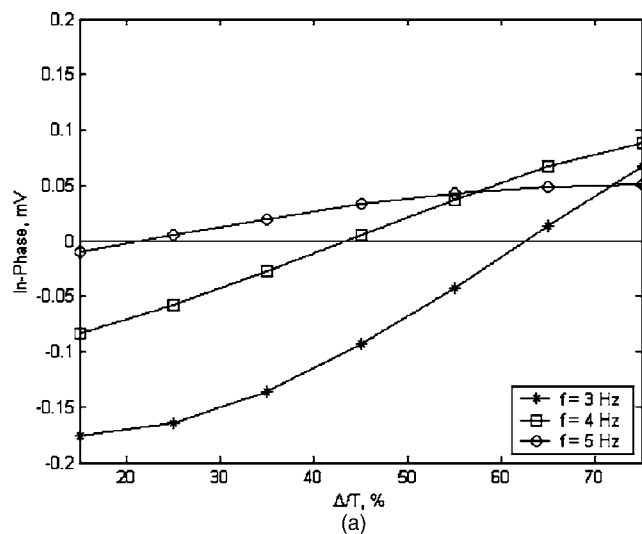


FIG. 6. (a) In-phase and (b) quadrature components of the common-mode-rejection demodulation signal in water for various modulation frequencies; cavity length  $L=0.5$  mm.

demodulation technique, 15 consecutive frequency scans were measured with a cavity length  $L=0.5$  mm. It was observed that the amplitude shifted substantially upward at the lower frequencies. However, in the frequency range of ca. 4–5 Hz the shift was relatively small. Based on these results, the optimum parameters for the common-mode-rejection demodulation measurements of water mixtures were chosen as follows: cavity length  $L=0.5$  mm and modulation frequency  $f=4$  Hz.

The resolution of the common-mode-rejection demodulation method was tested on different types of water (Fig. 7). The difference between signals is clearly seen for each sample, which can be explained by the presence of different kinds of particulates or contaminants in the samples. For example, highly purified water (Microfluidics Laboratory, University of Toronto, Canada) is significantly different from tap water samples from both Canada and Greece (Fig. 7).

Typical common-mode-rejection demodulation scans for water-methanol and water-ethanol mixtures are presented in Figs. 8 and 9, respectively. The experiments consisted of

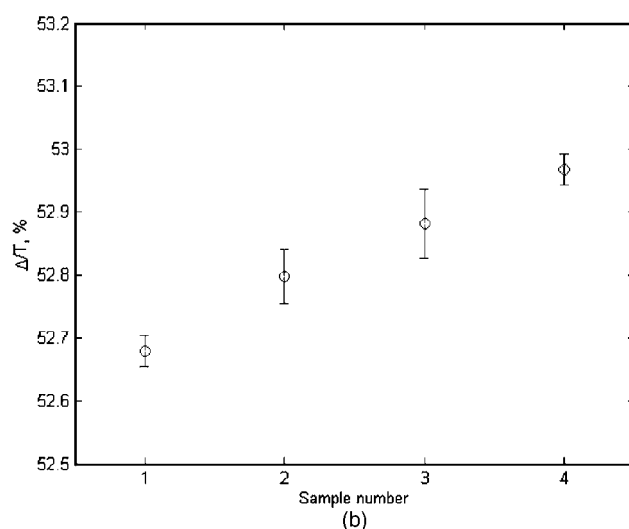
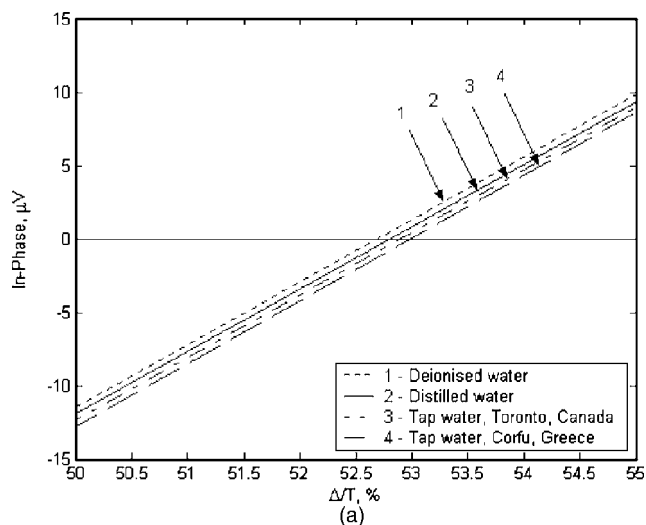


FIG. 7. (a) Averaged in-phase components of the signal for different water samples; (b) crossing points vs concentration;  $L=0.5$  mm,  $T=295$  K,  $f=4$  Hz,  $\tau_1/T=0.05$ ,  $\tau_2/T=0.25$ .

consecutive runs of four identical samples of concentrations 0%, 0.2%, 0.5%, and 1% v/v. The zero crossing percentage  $\Delta/T$  of the average results (mean of four measurements for the samples of the same concentration) clearly shows the difference in the in-phase signal for different concentrations of alcohol [Figs. 8(a) and 9(a)]. The thermal diffusivities [Figs. 8(b) and 9(b)], calculated according to the theoretical expressions [Eqs. (1a) and (2a)], show that the common-mode-rejection demodulation technique can attain resolution up to 0.2% v/v (0.16% w/w) concentration of methanol and ethanol in water.

The high-temperature stability of the developed method can be seen in Fig. 10 in which two successive measurements are shown. The first set was performed with the concentrations of ethanol in water in increasing order from 0% to 2% v/v. The second set was measured immediately afterwards, with the concentrations 0.5%, 0.2%, and 0% v/v, in decreasing order. It is seen that the results for the same concentrations are very close in both directions.

Overall, we found that the use of thermal-wave common-mode-rejection demodulation wave forms with the

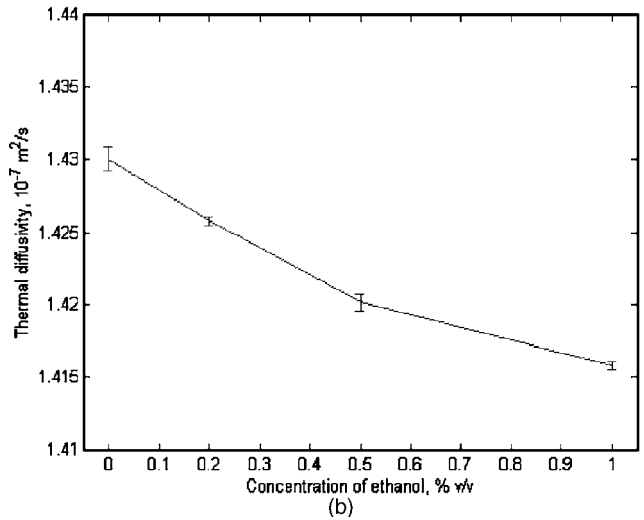
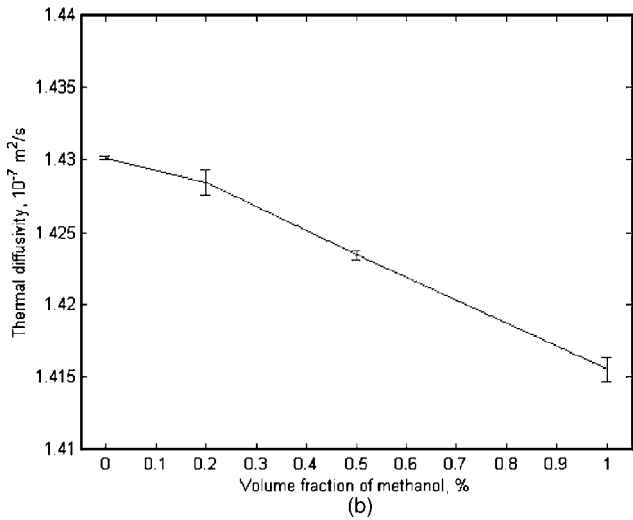
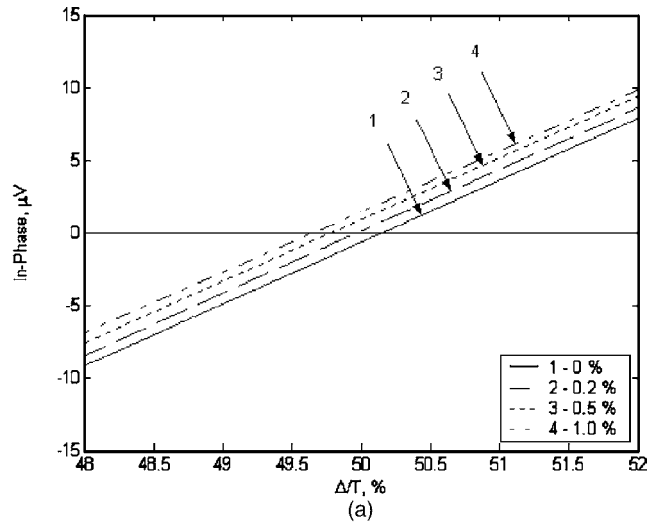
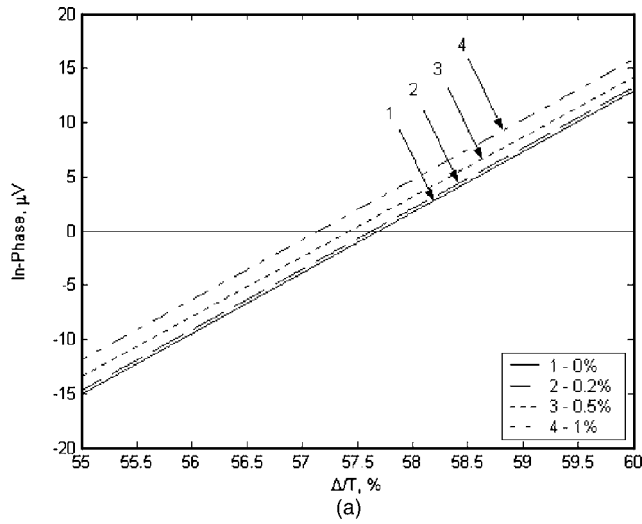


FIG. 8. (a) Averaged in-phase components of the signal for several concentrations of methanol; (b) thermal diffusivity vs concentration;  $L=0.5$  mm,  $T=293$  K,  $f=4$  Hz,  $\tau_1/T=0.05$ ,  $\tau_2/T=0.25$ . The thermal parameters used in calculations are presented in Table I.

FIG. 9. (a) Averaged in-phase components of the signal for several concentrations of ethanol; (b) thermal diffusivity vs concentration;  $L=0.5$  mm,  $T=293$  K,  $f=4$  Hz,  $\tau_1/T=0.05$ ,  $\tau_2/T=0.25$ . The thermal parameters used in calculations are presented in Table I.

pyroelectric cavity sensor is able to measure thermal diffusivity of water-alcohol mixtures at the level of 0.2% v/v (0.16% w/w).

Photopyroelectric frequency scans using a thermal-wave cavity and a theoretical conduction-radiation model were shown to be a robust technique for the determination of thermal diffusivity of water mixtures. The advantage in measurement using common-mode-rejection demodulation method over frequency-scan thermal-wave detection techniques is that common-mode-rejection demodulation involves a single modulation frequency (i.e., no signal normalization is needed) and fixed cavity length (i.e., mechanical hysteresis of moving parts is avoided). The frequency-scan measurements exhibited maximum resolution of the photothermal signal in water at the level of 0.5% by volume in mixtures of methanol and ethanol. The common-mode-rejection demodulation method improved the resolution up to the level of 0.2% by volume for the reasons stated above. To our best knowledge, this is the highest thermophysical resolution of water-methanol and water-ethanol mixtures reported to date.

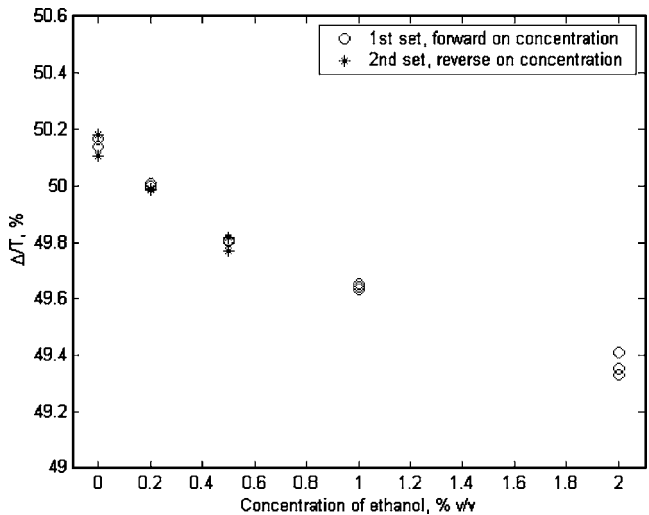


FIG. 10. Crossing points vs concentration of ethanol in water, forward and reverse sets of measurements.

Moreover, the common-mode-rejection demodulation technique allows direct calculation of thermal-diffusivity values based on the zero crossings of the in-phase and quadrature signal channels, instead of complicated fitting procedures used for frequency-scan experimental data. The ultrahigh sensitivity of the method can be especially useful in environmental applications, specifically in real-time water pollution monitoring.

#### ACKNOWLEDGMENT

The support of the Natural Sciences and Engineering Research Council of Canada (NSERC) is gratefully acknowledged.

- <sup>1</sup>D. Comeau, A. Hache, and N. Melikchi, *Appl. Phys. Lett.* **83**, 246 (2003).
- <sup>2</sup>J. A. P. Lima, E. Marin, M. S. O. Massunaga, O. Correa, S. L. Cardoso, H. Vargas, L. C. M. Miranda, *Appl. Phys. B* **73**, 151 (2001).
- <sup>3</sup>J. Wang and M. Fiebig, *Int. J. Thermophys.* **16**, 1353 (1995).
- <sup>4</sup>J. Wang and M. Fiebig, *Int. J. Thermophys.* **19**, 15 (1998).
- <sup>5</sup>J. Wang and M. Fiebig, *Int. J. Thermophys.* **21**, 35 (2000).
- <sup>6</sup>J. A. Balderas-Lopez, A. Mandelis, and J. A. Garcia, *Rev. Sci. Instrum.* **71**, 2933 (2000).
- <sup>7</sup>A. Matvienko and A. Mandelis, *Int. J. Thermophys.* **26**, 837 (2005).
- <sup>8</sup>J. Shen and A. Mandelis, *Rev. Sci. Instrum.* **66**, 4999 (1995).
- <sup>9</sup>J. A. Balderas-Lopez and A. Mandelis, *J. Appl. Phys.* **90**, 3296 (2001).
- <sup>10</sup>A. Mandelis, S. Paoloni, and L. Nicolaidis, *Rev. Sci. Instrum.* **71**, 2440 (2000).
- <sup>11</sup>S. Paoloni, L. Nicolaidis, and A. Mandelis, *Rev. Sci. Instrum.* **71**, 2445 (2000).
- <sup>12</sup>J. P. Holman, *Heat Transfer*, 7th ed. (McGraw-Hill, New York, 1990).
- <sup>13</sup>R. C. Reid, J. M. Prausnitz, and T. K. Sherwood, *The Properties of Gases and Liquids* (McGraw-Hill, New York, 1977), p. 533.